

# Charge Translocation Coupled to Electron Injection into Oxidized Cytochrome *c* Oxidase from *Paracoccus denitrificans*<sup>†</sup>

Michael I. Verkhovsky,\* Anne Tuukkanen, Camilla Backgren, Anne Puustinen, and Mårten Wikström\*

Department of Medical Chemistry, Institute of Biomedical Sciences and Biocentrum Helsinki, P.O. Box 8, 00014 University of Helsinki, Helsinki, Finland

Received January 4, 2001

**ABSTRACT:** Electrons were discretely injected into oxidized cytochrome *c* oxidase in liposomes by laser flash excitation of bound ruthenium [II] bispyridyl, and the membrane potential was recorded by time-resolved electrometry. Membrane potential is generated in a fast phase when an electron is transferred from the excited dye, via the Cu<sub>A</sub> center, to heme *a* at a relative dielectric depth *d* inside the membrane [Zaslavsky, D., Kaulen, A. D., Smirnova, I. A., Vygodina, T., and Konstantinov, A. A. (1993) *FEBS Lett.* 336, 389–393]. Subsequently, membrane potential may develop further in a slower event, which is due to proton transfer into the enzyme from the opposite side of the membrane [Ruitenbergh, M., Kannt, A., Bamberg, E., Ludwig, B., Michel, H., and Fendler, K. (2000) *Proc. Natl. Acad. Sci. U.S.A.* 97, 4632–4636]. Here, we confirm that injection of the first electron into the fully oxidized cytochrome *c* oxidase from *Paracoccus denitrificans* is associated with a fast electrogenic 11 μs phase, but there is no further electrogenic phase up to 100 milliseconds when special care is taken to ensure that only fully oxidized enzyme is present initially. A slower electrogenic 135 μs phase only becomes apparent and grows in amplitude upon increasing the number of light flashes. This occurs in parallel with a decrease in amplitude of the 11 μs phase and correlates with the number of enzyme molecules that are already reduced by one electron before the flash. The electrogenic 135 μs phase does not appear with increasing flash number in the K354M mutant enzyme, where electron and proton transfer into the binuclear center is delayed. We conclude that the 135 μs phase, and its associated proton uptake, take place on electron injection into enzyme molecules where the binuclear heme *a*<sub>3</sub>–Cu<sub>B</sub> site is already reduced by one electron, and that it is accompanied by oxidation of heme *a* with a similar time constant. Reduction of heme *a* is not associated with electrogenic proton uptake into the enzyme, neither in the fully oxidized nor in the one-electron-reduced enzyme. The extent of the electrogenic 135 μs phase also rules out the possibility that reduction of the binuclear center by the second electron would be coupled to proton translocation in addition to the electrogenic uptake of a proton.

Cytochrome *c* oxidase catalyses the respiratory reduction of dioxygen to water in the mitochondria of all eukaryotes and in many aerobic bacteria (for reviews, see refs 1 and 2). This redox activity is linked to separation of electrical charge across the mitochondrial or bacterial membrane, and to formation of a pH gradient, thus generating a protonmotive force across the membrane, which may be utilized for the synthesis of ATP catalyzed by a membrane bound H<sup>+</sup>-coupled ATP synthase. Cytochrome *c* oxidase has four redox-active metal centers. The bimetallic Cu<sub>A</sub> center in subunit II accepts electrons from the donor, cytochrome *c*, and resides outside the dielectric barrier of the membrane. The low spin heme *a* in subunit I accepts electrons from Cu<sub>A</sub> and resides inside the membrane domain (3, 4) at a relative dielectric distance *d* from the positively charged *P*-side (Figure 1). The binuclear heme *a*<sub>3</sub>–Cu<sub>B</sub> center, also in subunit I, receives

electrons from heme *a* and lies at approximately the same depth *d* within the dielectric. This is the site that binds O<sub>2</sub> and catalyses its reduction to water. The catalytic cycle of cytochrome *c* oxidase has been extensively elucidated by time-resolved spectroscopic techniques (1, 2), and the linkage of individual catalytic steps to proton and charge translocation has been studied in reconstituted proteoliposomes by pH measurements, as well as by time-resolved electrometry (5–8).

O<sub>2</sub> reacts with the binuclear heme *a*<sub>3</sub>–Cu<sub>B</sub> site as soon as the oxidized ferric-cupric site (**O** state) has been reduced to the ferrous-cuprous form **R** by two electrons in the *reductive phase* of the catalytic cycle. This *reductive phase* is also associated with net uptake of two protons into the enzyme from the N-side of the membrane (9, 10). In the subsequent *oxidative phase*, the reaction of **R** with O<sub>2</sub> first produces the ferrous heme *a*<sub>3</sub>–O<sub>2</sub> adduct, **A** (1, 2, 11). If no further electrons are available in either heme *a* or Cu<sub>A</sub>, compound **A** decomposes into the so-called **P<sub>M</sub>** intermediate (originally called compound C; ref 11), with a characteristic time constant of ca. 200 μs at room temperature (1, 2), with scission of the O–O bond, oxidation of ferrous heme *a*<sub>3</sub> into

<sup>†</sup> Supported by grants from Biocentrum Helsinki, the Academy of Finland (program 44895), the University of Helsinki, and the Sigrid Juselius Foundation.

\* To whom correspondence should be addressed. (M.I.V.) E-mail: Michael.Verkhovsky@Helsinki.Fi. (M.W.) Marten.Wikstrom@Helsinki.Fi. Fax: +358-9-191 8296.

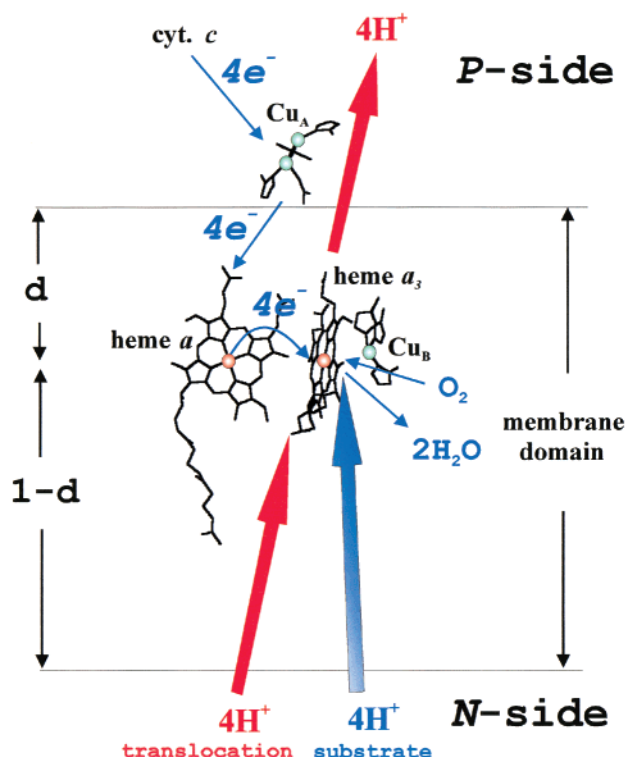


FIGURE 1: Scheme of cytochrome *c* oxidase in the membrane (adapted from ref 8). Heme *a* and the binuclear heme  $a_3$ –Cu<sub>B</sub> center lie at a relative dielectric depth *d* inside the membrane, whereas the Cu<sub>A</sub> center lies outside the membrane dielectric on the positively charged *P*-side of the membrane. The scheme shows the overall reduction of O<sub>2</sub> to two water molecules at the binuclear center, linked to uptake of four electrons from the donor, cytochrome *c*, and of four protons from the negatively charged *N*-side of the membrane (blue arrow). The overall reaction is further linked to translocation of four protons across the membrane (red arrows). In reality, cytochrome *c* donates one electron at the time to the binuclear site, via Cu<sub>A</sub> and heme *a*, which gives rise to oxygen intermediates at the O<sub>2</sub> reduction site during the catalytic cycle (see text).

its ferryl form, and oxidation of Cu<sub>B</sub> (12). The fourth electron equivalent is either taken from a tyrosine residue in the vicinity with formation of a neutral tyrosine radical (13), or alternatively Cu<sub>B</sub> is oxidized to Cu[III]. Input of a third electron, via Cu<sub>A</sub> and heme *a*, converts the **P<sub>M</sub>** state into the intermediate **F** with ferryl heme iron and cupric Cu<sub>B</sub>, and the fourth electron converts **F** back into the oxidized, ferric/cupric form **O** of the binuclear site via a metastable form of the **O** state (8).

The conversion of compound **A** into the **P<sub>M</sub>** state is not associated with translocation of electrical charge across the membrane (7), nor with net proton uptake (14). Transformation of the **P<sub>M</sub>** state to **F** and of **F** to **O** are each linked to net uptake of one proton from the *N*-side (14) and to translocation of one proton across the membrane (8). The issue to be addressed here is the extent and mechanism by which the *reductive phase* from state **O** to state **R** is linked to translocation of electrical charge, and this will be addressed by discrete photoinjection of electrons into the oxidized enzyme (15) and recording the translocation of charge electrometrically.

It has previously been reported that injection of the first electron into the oxidized enzyme results in a fast electro-metric response ( $\tau = 10\text{--}40\ \mu\text{s}$ , depending on the source of

enzyme) that may be attributed to electron transfer from the excited dye to heme *a*, via Cu<sub>A</sub>, across *d* of the dielectric (see Figure 1; refs 5 and 6). Ruitenbergh et al. (16) and ourselves (17) working with the *P. denitrificans* enzyme reported that this fast phase is followed by a slower electrogenic phase ( $\tau \approx 150\ \mu\text{s}$ ) that was attributed to proton uptake into the binuclear site from the *N*-side of the membrane. This proton uptake was interpreted to be either a response to the reduction of heme *a* (16), or due to reduction of the binuclear site (17). However, Siletsky et al. (18) did not observe such a phase in the bovine enzyme and only reported a much slower millisecond electrogenic phase that they attributed to small amounts of enzyme molecules in the **F** or **P** states. The experiments to be reported here resolve this apparent discrepancy and show that only the fast electrogenic phase due to electron transfer to heme *a* is observed after the first flash when special care is taken to keep the enzyme initially in the fully oxidized state. Comparison of the experimental results with statistical modeling shows that the reduction of heme *a* is not associated with electrogenic proton uptake into the fully oxidized or the one-electron-reduced enzyme. This finding is inconsistent with those models of proton translocation by cytochrome *c* oxidase, which postulate that electrogenic uptake of the proton to be pumped is linked to reduction of heme *a* (19–24).

## MATERIALS AND METHODS

**Reagents.** The phospholipid for preparation of proteoliposomes and for the electrometric measuring membranes was L-lecithin, type IV-S (soybean, Sigma). Catalase (bovine liver) was from Sigma. RuBiPy<sup>1</sup> (tris[2,2'-bipyridyl]ruthenium[II] chloride hexahydrate) was from Aldrich.

**Enzymes and Proteoliposomes.** Cytochrome *c* oxidase from *Paracoccus denitrificans* was isolated and purified, and the K354M mutation in subunit I of this enzyme was introduced as described previously (25). Both wild-type and mutant enzyme was incorporated into proteoliposomes by the method introduced by Rigaud et al. (26), using Bio-Beads SM-2 adsorbent (Bio-Rad), as applied for cytochrome *c* oxidase (7), with small modifications. The sucrose gradient was omitted, and in order to increase the signal, the enzyme-to-lipid ratio was increased. The basic solution with 100 mM HEPES (pH 7.5), 2% (w/v) potassium cholate, and 160 mg of phospholipid was sonicated and centrifuged. Either 0.27 mL of 50  $\mu\text{M}$  wild-type enzyme or 0.19 mL of 140  $\mu\text{M}$  K354M mutant enzyme was added to 2 mL of this solution.

**Measurement Procedure.** The direct, time-resolved electrometric measurement is based on a method originally developed for bacterial reaction centers and bacteriorhodopsin by Drachev et al. (27) and applied later for cytochrome *c* oxidase (5). In the present system, Ag/AgCl<sub>2</sub> electrodes (World Precision Instruments, Stevenage, Hertfordshire, U.K.) record the voltage between the two compartments of a cell separated by a measuring membrane. The latter consists of a lipid-impregnated Teflon mesh (7, 28).

**Sample Preparation.** A total of 20  $\mu\text{L}$  of proteoliposome solution was added to one of the two compartments of the

<sup>1</sup> Abbreviations: RuBiPy, tris[2,2'-bipyridyl]ruthenium [II]; *k*, rate constant;  $\tau$ , time constant ( $1/k$ ).

cell and the proteoliposomes were fused to the measuring membrane by 12 mM CaCl<sub>2</sub>, which was added to both compartments, followed by a 2 h incubation at pH 7 (100 mM MOPS). Then, the liquid in both compartments was exchanged for 2 mM buffer (usually HEPES, pH 8) with 10 mM aniline. RuBiPy was added at the last moment in the dark and the sample was then carefully kept in the dark all the time before the experiment. Finally, the Ag/AgCl<sub>2</sub> electrodes were inserted, and a laser flash (Quantel Brilliant, frequency doubled YAG; pulse energy 180 mJ) started the reaction. Individual flashes were separated by 8 s.

**Measurement Electronics.** The measurement system consisted of a homemade operational preamplifier the output of which was recorded using an IBM-PC-based digitizer, a 12 bit CompuScope 512 (Gage Applied Sciences, Montreal, Canada), running data acquisition software written by Nikolai Belevich. A CTM-05 counter-timer board (Metrabyte) controlled timing.

## RESULTS

**Rationale.** Fully oxidized cytochrome *c* oxidase can take up four electrons, one each in the Cu<sub>A</sub> center and heme *a*, and two in the binuclear heme *a*<sub>3</sub>–Cu<sub>B</sub> site (Figure 1). Flash-induced photoreduction of the enzyme using ruthenium [II] bispyridyl (RuBiPy) essentially introduces either one or no electron into an enzyme molecule per flash because the quantum yield is low (15). Statistical analysis shows that with multiple flash excitation in such a system and with injection of the same quantity (*x*) of electrons per flash, the fraction of enzyme molecules with *m* electrons after *n* flashes is

$$\frac{\prod_{i=1}^m (n - i + 1)}{m!} x^m (1 - x)^{n-m} \quad (1)$$

The fractional extent by which an *m*-electron-reduced state is formed upon the *n*th flash is

$$\frac{\prod_{i=1}^{m-1} (n - i)}{(m - 1)!} x^m (1 - x)^{n-m} \quad (2)$$

This is shown in Figure 2 for the one-, two-, three-, and four-electron-reduced states as a function of flash number (*n*), and with an arbitrarily assumed quantum yield of 0.06. As the figure shows, the extent by which the one-electron-reduced state appears is largest on the first flash and then decreases by increasing flash number. In contrast, the extent by which the two-electron-reduced state appears is zero on the first flash, and then steadily increases and saturates around the 20th flash, whereas the three- and four-electron-reduced states appear much more slowly.

In the experimental setup, however, the enzyme is in an aerobic milieu and is therefore expected to behave somewhat differently. The two-electron-reduced enzyme will react with O<sub>2</sub> and form the **P<sub>M</sub>** state. The three-electron-reduced enzyme will form the **F** state, and the four-electron-reduced enzyme will regenerate the fully oxidized **O** state. However, as seen from Figure 2, the three- and four-electron-reduced states

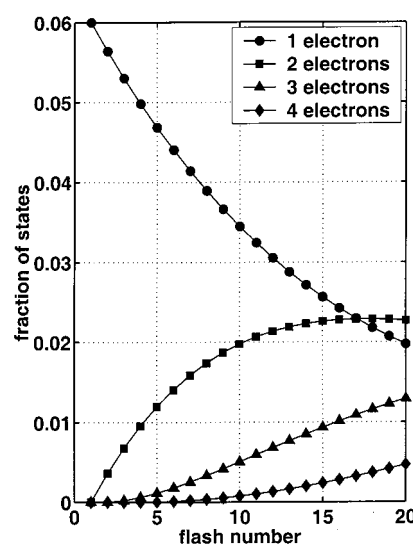


FIGURE 2: Formation of differently reduced states of the enzyme upon successive laser flashes. The extent by which one-, two-, three-, and four-electron-reduced states are formed for each light flash was calculated according to eq 2, assuming a quantum yield of 0.06, except that the fact that the enzyme can take only four electrons has been accounted for. Thus, one-electron-reduced enzyme is the sum of the one-, five-, nine-, ..., electron-reduced states, two-electron-reduced enzyme is the sum of the two-, six-, 10-, ..., electron-reduced states, etc.

will be significantly formed only after a large number of light flashes, whereas formation of the one- and two-electron-reduced states will dominate the behavior during the first 10 flashes.

**Experimental.** It turned out to be essential to prepare the samples with extreme care to prevent the enzyme from becoming prereduced by one electron, especially in the presence of RuBiPy. Handling of the sample in the dark was found to be particularly important. Otherwise, already the first flash leads not only to the fast electrogenic phase but also to a subsequent slower electrogenic phase with substantial amplitude. Such a slower phase was indeed recently reported for the first flash by both Ruitenberget al. (16) and by ourselves (17). In our earlier experiment (17), sufficient care was not taken to prepare the sample in the dark. Ruitenberget al. (16) performed their experiment anaerobically in the presence of ferricyanide, but glucose and glucose oxidase were also present. We have found that glucose effectively reduces ferricyanide to ferrocyanide in the presence of glucose oxidase (not shown), which is not surprising considering that glucose oxidase is a soluble flavoprotein. This readily accounts for formation of a substantial fraction of one (or more)-electron-reduced enzyme in the sample prior to the laser flash.

Figure 3 shows the electrometric response upon the 1st, 5th, and 15th laser flash after careful sample preparation in the dark, for the wild-type (A) and the K354M mutant enzyme (B). In both cases, the first flash causes the fast electrogenic phase ( $\tau \approx 11 \mu\text{s}$ ), but there is no subsequent electrogenic phase within some 100 ms. In the wild-type enzyme, a slower phase with  $\tau \approx 135 \mu\text{s}$  grows in only on subsequent flashes and increases in amplitude with flash number, while the fast phase simultaneously diminishes in amplitude (see below). In agreement with ref 16, we observed no 135  $\mu\text{s}$  phase with the mutant enzyme, only a decrease in amplitude of the fast phase with increasing flash number.



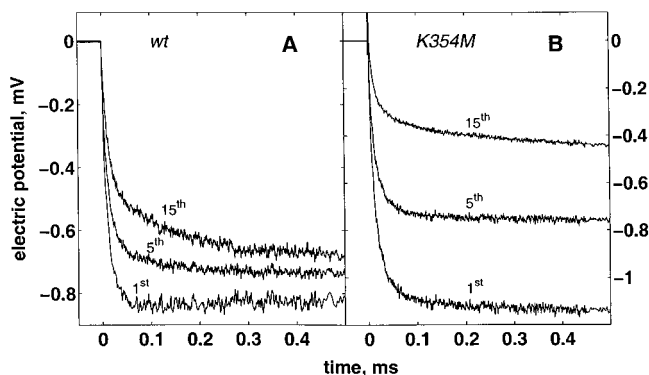


FIGURE 3: Kinetic curves of electric potential generation in wild-type (A) and K354M mutant (B) cytochrome *c* oxidase upon flash-induced electron injection into oxidized enzyme. Both panels show the traces recorded on the 1st, 5th, and 15th flash. Zero time corresponds to the time the laser flash was fired. 2 mM HEPES buffer (pH 8), 80  $\mu$ M RuBiPy, 10 mM aniline (for details, see Materials and Methods).

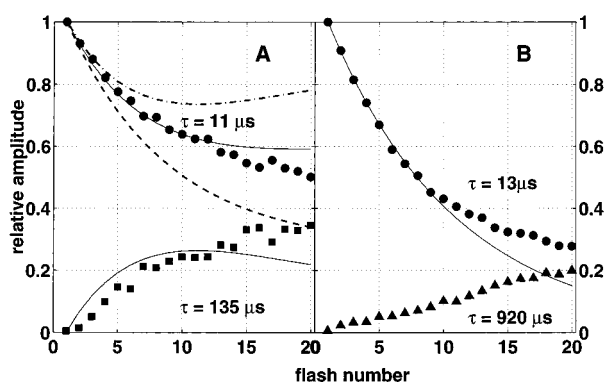


FIGURE 4: Dependence of the amplitude of the different kinetic phases of potential generation on flash number in wild-type (A) and K354M (B) mutant cytochrome *c* oxidase. Conditions as for Figure 2. The amplitudes and rate constants were obtained by global exponential fitting of the complete set of 20 flashes. The curves in panel A were generated by a model as described in the text and in the legend of Figure 6. The first injected electron is assumed always to be fully transferred from  $\text{Cu}_A$  to heme *a*. 100% (— · — · —), 70% (solid lines), and 30% (— — —) of the second, third, and fourth electron injected is assumed to be transferred from  $\text{Cu}_A$  to heme *a*, respectively. The curve in panel B was generated by assuming that the electron injected into heme *a* will never equilibrate with the binuclear center (see text).

A slow electrogenic phase ( $\tau \approx 920 \mu\text{s}$ ) with small amplitude appeared in the mutant enzyme after several flashes (see ref 16 and below).

A global exponential fit of 20 flashes yielded the time constants ( $\tau$ ) and amplitudes for the two phases. The amplitudes are shown as a function of flash number in Figure 4 for the wild-type and mutant enzymes. It can be seen immediately that in the wild-type enzyme the dependence of the amplitude of the two phases on flash number follows qualitatively quite well the predicted appearance of one-electron and two-electron-reduced states, respectively (cf. Figure 2).

In the mutant enzyme (Figure 4B), the amplitude of the fast phase decreases more steeply with flash number. The millisecond phase ( $\tau = 920 \mu\text{s}$ ) seen here (cf., ref 16) increases only very slowly in amplitude with flash number, a pattern that may fit the appearance of some three-electron-reduced state. We have indeed observed a phase of mem-

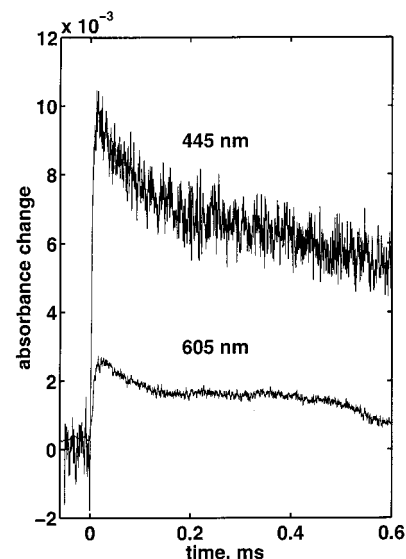


FIGURE 5: Absorbance changes in soluble oxidized wild-type cytochrome *c* oxidase from *P. denitrificans* caused by electron injection by photoexcitation of RuBiPy. Tricine buffer (2 mM, pH 8), 40  $\mu$ M RuBiPy, 10 mM aniline, 25  $\mu\text{g}/\text{mL}$  catalase, 0.05% (w/w) dodecyl maltoside, and 2  $\mu\text{M}$  cytochrome *c* oxidase. The curves at 445 and 605 nm were obtained by averaging 50 flashes.

brane potential generation with a similar time constant upon photoinjection of an electron into the K354M mutant enzyme in the F state (not shown). Photoreduction of bovine enzyme with the binuclear center in the F state has also been previously shown to yield an electrogenic response in the millisecond range (18), and the mutation corresponding to K354M in the *Rhodobacter sphaeroides* enzyme has been shown not to significantly affect the oxidative phase of the catalytic cycle, its associated proton uptake (29) or generation of membrane potential (6).

We may now attempt to fit the observed pattern of membrane potential generation to two models that may be proposed to explain the 11 and 135  $\mu\text{s}$  phases. In both models, the 11  $\mu\text{s}$  phase is due to electron transfer from  $\text{Cu}_A$  to heme *a*, as first shown by Konstantinov et al. (5), and which occurs across *d*, the relative dielectric depth at which heme *a* and the binuclear center reside inside the membrane (Figure 1). Ruitenber et al. (16) suggested that heme *a* reduction by the first electron leads to uptake of a proton from the N-side of the membrane to a site near the binuclear center, and that this causes the 150  $\mu\text{s}$  (here 135  $\mu\text{s}$ ) electrogenic phase. In contrast, we have proposed that this phase results from proton uptake in response to electron transfer from heme *a* to the binuclear site and that the reduction of heme *a* is not as such linked to proton uptake (17). Optical data have shown that the first electron does not equilibrate with the binuclear site within a millisecond (15, 30, 31), and we show here that the 135  $\mu\text{s}$  phase is not present at all after injection of the first electron (Figures 3 and 4). Therefore, we suggest that within the time span studied here, electron equilibration between heme *a* and the binuclear center only occurs in the two-electron-reduced enzyme. In agreement with this, such fast reoxidation of heme *a* is not observed for the first electron (15, 30, 31), but it is indeed observed after multiple flashes as shown in Figure 5, where the oxidation of heme *a* was measured optically at 605 and 445 nm, and with kinetics that resemble the electrogenic 135  $\mu\text{s}$  phase. This confirms and extends

our earlier observation of partial reduction of the binuclear center within a millisecond under such conditions, based on changes in the optical absorption spectrum (17).

**Modeling.** The amplitude of the fast phase on the first flash ( $a_1$ ) can be described as

$$a_1 = xdQ \quad (3)$$

where  $x$  is the quantum yield,  $d$  is the relative dielectric depth of heme  $a$  in the membrane (Figure 1), and  $Q$  is the potential created by translocation of a single charge across the entire dielectric. This assumes that the electron is completely transferred from  $\text{Cu}_A$  to heme  $a$ , which is reasonable considering the much higher midpoint potential of heme  $a$ . The amplitude of the fast phase upon the second flash ( $a_2$ ) will depend on the fraction ( $\alpha$ ) by which heme  $a$  was oxidized by the binuclear center between the first and the second flashes. In this case, we can no longer assume that the electron is fully transferred from  $\text{Cu}_A$  to heme  $a$ , because the midpoint potential of the latter has been significantly lowered by the anticooperative redox interaction with the binuclear site. This is accounted for here by the parameter  $\beta$ , which is the fraction by which the second electron is transferred from  $\text{Cu}_A$  to heme  $a$ . Thus

$$a_2 = [x(1-x) + \alpha\beta x^2]dQ \quad (4)$$

If the equilibration of the first electron with the binuclear center were hindered, either thermodynamically or kinetically, the amplitude of the fast phase would be expected to decrease more steeply with flash number. Such a change is indeed observed in the K354M mutant enzyme (Figure 4B), which thus indicates hindrance for the first electron to equilibrate between heme  $a$  and  $\text{Cu}_B$ . Heme  $a_3$  reduction has been shown to be strongly inhibited in this mutant enzyme (17, 32, 33), but Jünemann et al. (34) have reported that  $\text{Cu}_B$  does become at least partially reduced after the first electron. However, there is little information on the rate of this process.

As shown by the curve in Figure 4B, the behavior expected for lack of equilibration of the first electron with the binuclear site is followed during several flashes in the mutant enzyme, but eventually some equilibration does occur after ca. nine flashes. This experiment shows, in agreement with Jünemann et al. (34), that equilibration of the electron at heme  $a$  with the binuclear site ( $\text{Cu}_B$ ) does occur even in the mutant enzyme, albeit much more slowly than in the wild-type.

With no equilibration of the first electron between heme  $a$  and  $\text{Cu}_B$ , the parameter  $\alpha$  would be zero and the ratio of the amplitudes of the fast phases after the two first flashes would give the quantum yield

$$x = 1 - a_2/a_1 \quad (5)$$

Assuming  $\alpha = 0$  for Figure 4B gives a quantum yield of 0.09 for the mutant enzyme. By assuming the same quantum yield for the wild-type enzyme, we may calculate the product  $\alpha\beta$  from  $a_1$  and  $a_2$  in the wild-type enzyme (Figure 4A),

$$\alpha\beta = 1 - (1 - a_2/a_1)/x \quad (6)$$

This yields  $\alpha\beta = 0.24$ , which is proportional to the product of the equilibrium constants of electron transfer between  $\text{Cu}_B$  and heme  $a$  and  $\text{Cu}_A$  and heme  $a$ , respectively (see below).

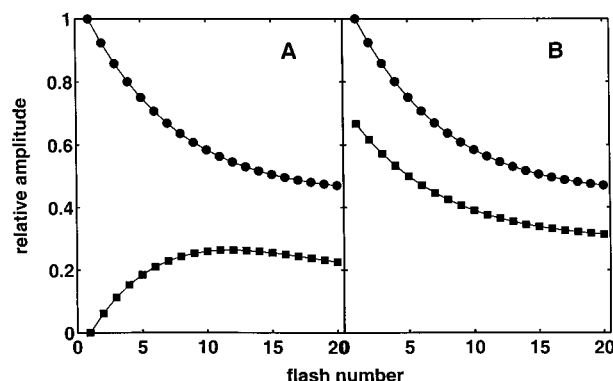


FIGURE 6: Predicted behavior of the amplitudes of the electrogenic 11  $\mu\text{s}$  (●) and 135  $\mu\text{s}$  (■) phases on flash number according to two different assignments of the 135  $\mu\text{s}$  phase. In both models A and B, the fast phase is due to electron transfer from the excited dye into heme  $a$ , across  $d$  of the dielectric (Figure 1), and the first electron equilibrates among heme  $a$  and  $\text{Cu}_B$  between the light flashes, as defined by a 20 mV higher midpoint potential for heme  $a$ . Quantum yield 0.09 (see text). Model A: the 135  $\mu\text{s}$  phase reflects uptake of one proton from the N-side of the membrane to the binuclear site, across  $1 - d$  of the dielectric [ $d = 0.32$  (ref 8)], on injection of the second electron into the fraction of enzyme where one electron is already located at  $\text{Cu}_B$  (cf., solid curves in Figure 4). Model B: the 135  $\mu\text{s}$  phase reflects uptake of one proton from the N-side of the membrane to the binuclear site, across  $1 - d$  of the dielectric (where  $d = 0.6$ ), and is a result of the reduction of heme  $a$ , as suggested by Ruitenber et al. (16). Hence, in this model the amplitude of the 135  $\mu\text{s}$  phase is always two-thirds of the amplitude of the 11  $\mu\text{s}$  phase.

The electrogenic 135  $\mu\text{s}$  phase is found here to correlate exclusively with formation of two-electron-reduced enzyme, i.e., with the injection of the second electron. In our model (Figure 6A), also shown as solid curves in Figure 4A, the amplitudes of the 11 and 135  $\mu\text{s}$  phases were calculated with the assumption that the 135  $\mu\text{s}$  proton uptake, concomitant with formation of the two-electron-reduced enzyme, occurs from the N-side of the membrane into the binuclear site, and across  $1 - d$  of the dielectric, where  $d = 0.32$  (8). Our model further assumes that the *first* electron will be transferred quantitatively from  $\text{Cu}_A$  to heme  $a$  due to the much higher midpoint potential of the latter in this case. However, for the case where the first electron is already at  $\text{Cu}_B$ , we must account for the effect of the anticooperative redox interaction between this center and heme  $a$  on the behavior of the second electron (cf. above). In Figure 4A, we have plotted three cases: (i) the second electron goes quantitatively to heme  $a$  ( $\beta = 1$ ), (ii) by a fraction ( $\beta$ ) of 0.3 or (iii) 0.7, respectively, the rest remaining on  $\text{Cu}_A$ . These three cases correspond to a much higher ( $>100$  mV) midpoint potential of heme  $a$  relative to  $\text{Cu}_A$  or to a 22 mV lower ( $\beta = 0.3$ ), or 22 mV higher potential ( $\beta = 0.7$ ). The data are clearly best fitted by the latter assumption. It is important to note that our model cannot be fitted to the data if this known anticooperative redox interaction is neglected.

Having thus an experimentally determined estimate of  $\beta$  we can obtain  $\alpha$  from eq 6, which yields  $\alpha = 0.34$ . This corresponds to a 17 mV higher midpoint redox potential of heme  $a$  than of  $\text{Cu}_B$  with respect to the first electron, in good agreement with earlier reports (34). Hence, the relatively slow equilibration of the first electron between heme  $a$  and the binuclear center does occur in the wild-type enzyme within the 8 s between the light flashes in the present experiments.

Our model arbitrarily assumes that the  $\text{Cu}_A/\text{heme } a$  equilibrium position is the same on injecting the third and fourth electron as it is on injecting the second electron, i.e., in the cases where the electron is injected into the  $\mathbf{P}_M$  and  $\mathbf{F}$  states, respectively. This is probably an oversimplification, but it is necessary in the absence of data on this point. It should be noted that the deviation between model and data beyond the 12th flash for the amplitude of the 11  $\mu\text{s}$  electrometric response as a function of flash number (Figure 4) can easily be made to disappear if the redox equilibrium between heme  $a$  and  $\text{Cu}_A$  is assumed to shift somewhat more toward  $\text{Cu}_A$  when the third and fourth electron are injected (not shown).

The experimental and simulation data are quite similar, which shows that our model describes the experimental observations satisfactorily. The deviation between experimental and model points from the 13th flash onward (Figure 4A) also finds another simple explanation: The model assumes that the differently reduced states of the enzyme are not interconvertible. However, in the experiment, the states formed with two and three electrons ( $\mathbf{P}_M$  and  $\mathbf{F}$ , respectively) are not stable, but will both decompose spontaneously into the  $\mathbf{O}$  state on a seconds time scale. The amplitude of the fast phase (reduction of heme  $a$ ) is expected to be the same in the  $\mathbf{P}_M$ ,  $\mathbf{F}$ , and  $\mathbf{O}$  states of the enzyme, since heme  $a$  is oxidized (but see above regarding a possible variation in the  $\text{Cu}_A/\text{heme } a$  equilibrium). Therefore, the increased population of  $\mathbf{O}$  at the expense of the relatively unstable  $\mathbf{P}_M$  and  $\mathbf{F}$  states should not as such change the amplitude of the fast phase in the experiment relative to the model. However, when this excess of enzyme in the  $\mathbf{O}$  state receives one electron, an excess of one-electron-reduced state is produced, relative to the assumptions in the model. This is another plausible cause of the excessive decrease in the amplitude of the fast phase beyond ca. 13 flashes in Figure 4A, and this would also explain the increase in amplitude of the slow phase relative to the model.

Figure 6B shows the result expected from the Frankfurt model (16). While the fast phase behaves in the same way as in Figure 6A, the dependence of the amplitude of the 135  $\mu\text{s}$  phase on flash number is very different: the amplitude decreases with flash number in parallel with the decrease in amplitude of the fast phase, which is not consistent with the experimental observations (Figure 4A).

## DISCUSSION

When the two-electron-reduced enzyme is formed, it will under the present experimental conditions react quantitatively with  $\text{O}_2$  to form the  $\mathbf{P}_M$  state. This means that none of the two-electron-reduced enzyme will remain in a state where either  $\text{Cu}_B$ ,  $\text{Cu}_A$ , heme  $a_3$ , or heme  $a$  is reduced. Previous work has shown that reduction of the binuclear site is associated with uptake of ca. two protons and that its reaction with  $\text{O}_2$  to form the  $\mathbf{P}_M$  state is not associated with further proton uptake. It is also known that there is no electrogenic response associated with the reaction of the mixed valence, two-electron reduced, enzyme with  $\text{O}_2$  to form  $\mathbf{P}_M$  (see the introductory portion of this paper). Hence, the proton uptake detected by the electrogenic 135  $\mu\text{s}$  phase is associated with reduction of the binuclear site when it receives its second electron, before reacting with  $\text{O}_2$ . Our results suggest,

therefore, that the transfer of the second electron and proton to the binuclear site is considerably faster than the transfer of the first. Although this could be attributed to the subsequent reaction of the reduced site with  $\text{O}_2$ , this explanation is rendered unlikely because Ruitenbergh et al. (16) found the 135  $\mu\text{s}$  phase (in their case  $\tau \approx 150 \mu\text{s}$ ) under anaerobic conditions. Instead, the difference between the rates of equilibration of the first and second electron (and corresponding protons) with the binuclear center might reflect different rate constants of the so-called D- and K-pathways of proton transfer to the binuclear center (35). This is in line with our earlier report that reduction of the binuclear center is controlled by proton uptake (36). We agree with Ruitenbergh et al. (16) that the proton uptake associated with the first electron is likely to occur via the K pathway and that proton uptake associated with the second electron occurs via the D pathway (17). However, in contrast to ref 16, we attribute both these proton uptake events to be linked to reduction of the binuclear center, not to reduction of heme  $a$ .

Recently, we have shown that proton uptake via the K- and D-pathways is asymmetric during reduction of the binuclear site in the sense that the two proton-accepting groups do not readily communicate with one another (17). One may speculate that the D-pathway is nonfunctional ("closed") in the fully oxidized enzyme (6, 35), perhaps due to lack of a water molecule that may provide protonic linkage between the conserved glutamic acid 278 (numbering of subunit I from *P. denitrificans* cytochrome *aa3*) and the proton acceptor (37). Slow proton uptake via the K pathway, coupled to arrival of the first electron to the binuclear site, might produce such a water molecule and thus open the D pathway (17, 37). This may be the reason for the much faster (135  $\mu\text{s}$ ) proton uptake via the D pathway upon arrival of the second electron.

## CONCLUSIONS

Injection of the first electron into fully oxidized cytochrome *c* oxidase from *P. denitrificans* leads to reduction of heme  $a$  in an 11  $\mu\text{s}$  event, but this is not associated with electrogenic uptake of protons. The subsequent equilibration of the first electron with the binuclear center is a slow process (15, 30, 31), possibly limited by slow concomitant proton uptake via the K pathway. However, in the experiments reported here, it clearly has time to occur between the laser flashes in the wild-type enzyme, although it is not observed on the time scale of the present electrometric application.

The electrogenic 135  $\mu\text{s}$  phase is due to proton uptake associated with formation of two-electron-reduced enzyme. Optical data provide strong evidence for the conclusion that this latter proton uptake is also not coupled to reduction of heme  $a$ , but with electron transfer from heme  $a$  into the binuclear center. In some proton translocation models of cytochrome *c* oxidase it has been postulated that electrogenic uptake of the proton to be pumped is linked to reduction of heme  $a$  (19–24). The results presented here are not consistent with this, and favor the alternative view that proton uptake in the proton translocation mechanism is linked to electron transfer from heme  $a$  to the binuclear center (38). It has also been proposed that the transfer of the second electron to the binuclear center may be linked to proton translocation in

addition to the net uptake of a proton (24). The extent of the electrogenic 135  $\mu$ s phase observed here is not consistent with this proposal.

## ACKNOWLEDGMENT

We would like to thank Audrius Jasaitis for technical help and Nikolai Belevich for software design.

## REFERENCES

1. Babcock, G. T., and Wikström, M. (1992) *Nature* 356, 301–309.
2. Ferguson-Miller, S., and Babcock, G. T. (1996) *Chem. Rev.* 96, 2889–2907.
3. Iwata, S., Ostermeier, C., Ludwig, B., and Michel, H. (1995) *Nature* 376, 660–669.
4. Tsukihara, T., Aoyama, H., Yamashita, E., Tomizaki, T., Yamaguchi, H., Shinzawa-Itoh, K., Nakashima, R., Yaono, R., and Yoshikawa, S. (1996) *Science* 272, 1136–1144.
5. Zaslavsky, D., Kaulen, A. D., Smirnova, I. A., Vygodina, T., and Konstantinov, A. A. (1993) *FEBS Lett.* 336, 389–393.
6. Konstantinov, A. A., Siletsky, S., Mitchell, D., Kaulen, A., and Gennis, R. B. (1997) *Proc. Natl. Acad. Sci. U.S.A.* 94, 9085–9090.
7. Jasaitis, A., Verkhovsky, M. I., Morgan, J. E., Verkhovskaya, M. L., and Wikström, M. (1999) *Biochemistry* 38, 2697–2706.
8. Verkhovsky, M. I., Jasaitis, A., Verkhovskaya, M. L., Morgan, J. E., and Wikström, M. (1999) *Nature* 400, 480–483.
9. Mitchell, R., Mitchell, P., and Rich, P. R. (1992) *Biochim. Biophys. Acta* 1101, 188–191.
10. Capitanio, N., Vygodina, T., Capitanio, G., Konstantinov, A. A., Nicholls, P., and Papa, S. (1997) *Biochim. Biophys. Acta* 1318, 255–265.
11. Chance, B., Saronio, C., and Leigh, J. S. (1975) *J. Biol. Chem.* 250, 9226–9237.
12. Proshlyakov, D. A., Pressler, M. A., and Babcock, G. T. (1998) *Proc. Natl. Acad. Sci. U.S.A.* 95, 8020–8025.
13. Proshlyakov, D. A., Pressler, M. A., DeMaso, C., Leykam, J. F., DeWitt, D. L., and Babcock, G. T. (2000) *Science* (in press).
14. Mitchell, R., and Rich, P. R. (1994) *Biochim. Biophys. Acta* 1186, 19–26.
15. Nilsson, T. (1992) *Proc. Natl. Acad. Sci. U.S.A.* 89, 6497–6501.
16. Ruitenbergh, M., Kannt, A., Bamberg, E., Ludwig, B., Michel, H., and Fendler, K. (2000) *Proc. Natl. Acad. Sci. U.S.A.* 97, 4632–4636.
17. Wikström, M., Jasaitis, A., Backgren, C., Puustinen, A., and Verkhovsky, M. (2000) *Biochim. Biophys. Acta* 1459, 514–520.
18. Siletsky, S., Kaulen, A. D., and Konstantinov, A. A. (1999) *Biochemistry* 38, 4853–4861.
19. Artzatbanov, V. Y., Konstantinov, A. A., and Skulachev, V. P. (1978) *FEBS Lett.* 87, 180–185.
20. Papa, S., Capitanio, N., and Villani, G. (1998) *FEBS Lett.* 439, 1–8.
21. Rich, P. R. (1999) in *Frontiers of Cellular Bioenergetics* (Papa, S., Guerrieri, F., and Tager, J. M., Eds.) Kluwer Academic/Plenum Publishers, New York, pp 179–192.
22. Rich, P. R., Jünemann, S., and Meunier, B. (1998) *J. Bioenerg. Biomembr.* 30, 131–138.
23. Michel, H. (1998) *Proc. Natl. Acad. Sci. U.S.A.* 95, 12819–12824.
24. Michel, H. (1999) *Biochemistry* 38, 15129–15140.
25. Riistama, S., Laakkonen, L., Wikström, M., Verkhovsky, M. I., and Puustinen, A. (1999) *Biochemistry* 38, 10670–10677.
26. Rigaud, J.-L., Pitard, B., and Levy, D. (1995) *Biochim. Biophys. Acta* 1231, 223–246.
27. Drachev, L. A., Kaulen, A. D., Semenov, A. Yu., Severina, I. I., and Skulachev, V. P. (1979) *Anal. Biochem.* 96, 250–262.
28. Verkhovsky, M. I., Morgan, J. E., Verkhovskaya, M. L., and Wikström, M. (1997) *Biochim. Biophys. Acta* 1318, 6–10.
29. Brzezinski, P., and Ädelroth, P. (1998) *J. Bioenerg. Biomembr.* 30, 99–107.
30. Geren, L. M., Beasley, J. R., Fine, B. R., Saunders, A. J., Hibdon, S., Pielak, G. J., Durham, B., and Millett, F. (1995) *J. Biol. Chem.* 270, 2466–2472.
31. Zaslavsky, D., Sadoski, R. C., Wang, K., Durham, B., Gennis, R. B., and Millett, F. (1998) *Biochemistry* 37, 14910–14916.
32. Ädelroth, P., Gennis, R. B., and Brzezinski, P. (1998) *Biochemistry* 37, 2470–2476.
33. Vygodina, T. V., Pecoraro, C., Mitchell, D., Gennis, R. B., and Konstantinov, A. A. (1998) *Biochemistry* 37, 3053–3061.
34. Jünemann, S., Meunier, B., Gennis, R. B., and Rich, P. R. (1997) *Biochemistry* 36, 14456–14464.
35. Gennis, R. B. (1998) *Biochim. Biophys. Acta* 1365, 241–248.
36. Verkhovsky, M. I., Morgan, J. E. and Wikström, M. (1995) *Biochemistry* 34, 7483–7491.
37. Backgren, C., Hummer, G., Wikström, M. and Puustinen, A. (2000) *Biochemistry* 39, 7863–7867.
38. Wikström, M., Morgan, J. E., and Verkhovsky, M. I. (1998) *J. Bioenerg. Biomembr.* 30, 139–145.

BI010030U